

# The parietal architecture binding cognition to sensorimotor integration: a multimodal causal study

Luca Fonia,<sup>1,†</sup> Antonella Leonetti,<sup>2,†</sup> Guglielmo Puglisi,<sup>1</sup> Marco Rossi,<sup>1</sup> Luca Viganò,<sup>2</sup> Bianca Della Santa,<sup>1</sup> Luciano Simone,<sup>3</sup> Lorenzo Bello<sup>2</sup> and Gabriella Cerri<sup>1</sup>

<sup>†</sup>These authors contributed equally to this work.

## Abstract

Despite human's praxis abilities are unique among primates, comparative observations suggest that these cognitive motor skills could have emerged from exploitation and adaptation of phylogenetically older building blocks, namely the parieto-frontal networks sub-serving prehension and manipulation. Within this framework, investigating to which extent praxis and prehension-manipulation overlap and diverge within parieto-frontal circuits could help in understanding how human cognition shapes hand actions. This issue has never been investigated by combining lesion mapping and direct electrophysiological approaches in neurosurgical patients.

To this purpose, seventy-nine right-handed left-brain tumor patients candidate for awake neurosurgery were selected based on inclusion criteria. First, a lesion mapping was performed in the early post-operative phase to localize the regions associated to an impairment in praxis (imitation of meaningless and meaningful intransitive gestures) and visuo-guided prehension (reaching-to-grasping) abilities. Then, lesion results were anatomically matched with intraoperatively identified cortical and white matter regions, whose direct electrical stimulation impaired hand-manipulation task.

The lesion mapping analysis showed that prehension and praxis impairments occurring in early post-operative phase were associated to specific parietal sectors. Dorso-mesial parietal resections, including the superior parietal lobe and precuneus, affected prehension performance, while resections involving rostral intraparietal and inferior parietal areas affected praxis abilities (covariate clusters, 5000 permutations, CFWER  $p < 0.05$ ). The dorsal bank of the rostral intraparietal sulcus was associated to both prehension and praxis (overlap of non-covariate

1 clusters). Within praxis results, while resection involving inferior parietal areas affected mainly  
2 the imitation of meaningful gestures, resection involving intraparietal areas affected both  
3 meaningless and meaningful gesture imitation. In parallel, the intraoperative electrical stimulation  
4 of the rostral intraparietal and the adjacent inferior parietal lobe with their surrounding white matter  
5 during hand-manipulation task evoked different motor impairments, i.e. the arrest and clumsy  
6 patterns respectively.

7 When integrating lesion mapping and intraoperative stimulation results, it emerges that imitation  
8 of praxis gestures first depends on the integrity of parietal areas within the dorso-ventral stream.  
9 Among these areas, the rostral intraparietal and the inferior parietal area play distinct roles in praxis  
10 and sensorimotor process controlling manipulation. Due to its visuo-motor “attitude”, the rostral  
11 intraparietal sulcus, putative human homologue of monkey AIP, might enable the visuo-motor  
12 conversion of the observed gesture (direct pathway). Moreover, its functional interaction with the  
13 adjacent, phylogenetic more recent, inferior parietal areas might contribute to integrate the  
14 semantic-conceptual knowledge (indirect pathway) within the sensorimotor workflow,  
15 contributing to the cognitive up-grade of hand-actions.

16  
17 **Author affiliations:**

18 1 MoCA Laboratory, Department of Medical Biotechnology and Translational Medicine,  
19 Università degli Studi di Milano, Milano 20122, Italy

20 2 Neurosurgical Oncology Unit, Department of Oncology and Hemato-Oncology, Università degli  
21 Studi di Milano, Milano 20122, Italy

22 3 Department of medicine and surgery, Università Degli Studi di Parma, Parma 43125, Italy

23  
24 Correspondence to: Puglisi Guglielmo

25 Fratelli Cervi street, 93, 20054 Segrate MI, Italy

26 E-mail [guglielmo.puglisi@gmail.com](mailto:guglielmo.puglisi@gmail.com)

27 **Running title:** Parietal architecture for praxis gesture

1 **Keywords:** apraxia; motor cognition; sensorimotor integration; dorsal stream

## 2 **Introduction**

3 Praxis is the neurological process by which cognition directs motor action<sup>1,2</sup>. This process allows  
4 an abstract, conceptual and extremely flexible use of our hand sensorimotor repertoire, which is  
5 considered a hallmark of the human evolution. Praxis embraces several skills, from the ability to  
6 functionally interact with tools or pantomime their use (transitive actions), to imitation of  
7 meaningless and meaningful gestures (intransitive actions). These skills can be dramatically  
8 impaired following brain lesions resulting in the so-called *apraxia*, a deficit in the execution of  
9 purposive hand movements, not attributable to elementary motor and sensory disorders.

10 Converging comparative evidence suggests that phylogenetic old brain mechanisms subserving  
11 transitive actions, such as object prehension and manipulation, may represent the *building blocks*  
12 from which the human praxis abilities have emerged<sup>3-5</sup>. Specifically in this regard, humans and  
13 non-human primates share similar dorso-dorsal and dorso-ventral parieto-frontal streams for  
14 controlling distinct, although complementary, aspects of the hand-object oriented actions<sup>6,7</sup>. In  
15 humans, the presence of the *building blocks* and the parallel expansion of the frontal, parietal, and  
16 temporal areas<sup>8</sup> led to a significant sophistication of the sensorimotor repertoire, which represents  
17 the substrate fostering in humans a rapid cultural evolutionary process. Coherent with this view,  
18 fMRI studies showed that the hand-related parieto-frontal connectivity extends in humans to  
19 compose the so-called *praxis representation network* (PRN<sup>9,10</sup>). The human PRN is a large-scale,  
20 left-lateralized, temporo-parietal-frontal circuit claimed to be involved in translating conceptual  
21 and sensorimotor information into purposeful hand skilled acts (praxis), including transitive and  
22 intransitive hand gestures<sup>9,11</sup>. Pivotal lesion studies in stroke patients support the evidence that  
23 impairment of specific parietal and temporal sectors of this large-scale-pathway results in the onset  
24 of distinct apraxia symptoms<sup>12-15</sup>.

25 Overall, these results suggest that the exploitation and modification of the pre-existing parieto-  
26 frontal *building blocks* under the guidance of evolutionary processes<sup>16-18</sup> has been critical for the  
27 achievement of sophisticated and cognitive directed hand actions. Among them, intransitive  
28 “communicative” hand-arm gestures represent a distinguishing feature of humans with respect to  
29 the monkeys that hardly use their hand for such purposes<sup>19</sup>. Within this framework, investigating

1 to which extent the pathways subserving object-oriented actions (including visuo-guided  
2 prehension and object-manipulation) and the pathways subserving intransitive praxis gestures  
3 overlap and differentiate within the parieto-frontal circuits, seems crucial to disclose the neural  
4 mechanisms shaping the motor action based on high-level cognitive information.

5 To this aim, the present study was grounded in the clinical setup for patients undergoing awake  
6 neurosurgery for brain tumor resection allowing to use complementary causal approaches and  
7 specifically 1) the lesion symptom mapping (LSM) and 2) the intraoperative direct electrical  
8 stimulation (DES). Specifically in this study, the LSM was performed in the early post-operative  
9 (7 days post-surgery) phase to localize the brain regions associated to lower scores in praxis  
10 (imitation of meaningless and meaningful intransitive hand gestures) and prehension (reaching-to-  
11 grasping) performance. The regions highlighted by the LSM were then anatomically matched with  
12 cortical and white matter regions related to haptic hand-object manipulation identified  
13 intraoperatively with direct electrical stimulation (DES) within the same cohort of patients. The  
14 intraoperative hand-manipulation task (HMt) was performed without visual guidance in order to  
15 isolate and preserve mainly motor (and/or somatomotor) components of the parieto-premotor areas  
16 subserving hand manipulation functions<sup>20–26</sup>. Primary input to the rationale of this study has been  
17 the observation that the application of the intraoperative HMt actually turned out to reduce also  
18 long-term upper-limb ideomotor apraxia deficits. This observation suggests a close proximity  
19 between manipulation and praxis substrates, fostering the hypothesis that the exploitation of  
20 specific hand-related *building blocks* might be an important aspect for the emergence of cognitive  
21 praxis gestures as well as a relevant clinical tool guiding the intraoperative monitoring. However,  
22 even though the permanent apraxia was avoided, about 20% of patients suffered of transient  
23 ideomotor apraxia symptoms in the early post-operative phase<sup>20</sup>. These transient symptoms may  
24 be explained by the marginal impairment of the praxis-related neural substrates, possibly  
25 interleaved with motor and/or somatomotor object-manipulation substrates and/or lying in the  
26 tissue along the resection cavity's borders draw with the HMt. In particular, in the early post-  
27 operative phase, the resection borders undergo to a transient inflammation possibly altering their  
28 correct functioning.

29 Overall, these clinical considerations fostered the need to investigate the degree of co-localization  
30 between the intraoperative DES sites associated to HMt, and the regions associated to lower scores

1 in praxis functions in early post-operative phase. However, the intraoperative HMt involved only  
2 the distal control of the hand-object interaction, therefore the full deployment of the visuo-guided  
3 prehension (from the direction of arm movements to the shaping of the hand according to the object  
4 shape and location), i.e. reaching-to-grasping, was intraoperatively unexplored. To fill this gap and  
5 provide the most comprehensive view of all the areas involved in the hand-object oriented action  
6 (from proximal-reaching to distal-grasping/manipulation), the spatial matching between the  
7 regions associated to lower scores in visuo-guided prehension assessment and the intraoperative  
8 hand-manipulation-related sectors was performed. Notably, the complementary use of three tasks  
9 (HMt, visuo-guided prehension and praxis) all constrained to the dexterous use of the hand as a  
10 final common path, grounds on four pillars: 1) the tasks rely on different sensory and sensorimotor  
11 modalities: visuomotor (both prehension and praxis) and somatosensory-motor (or somatomotor,  
12 all the tasks); 2) the tasks investigated distinct hand-action domains: *transitive* hand-object  
13 oriented actions (HMt and prehension) and imitation of *intransitive* gesture (praxis); 3) within  
14 transitive action, the haptic execution of the HMt investigated the somatomotor component  
15 involved in the hand-object oriented action, while the visuo-guided prehension extended the  
16 investigation to the visuomotor component; 4) within praxis, gestures to be imitated differed in the  
17 cognitive content: communicative (meaningful) or not (meaningless).

18 The combined use of the tasks along the four pillars allowed to investigate the degree of co-  
19 localization between the areas involved in *transitive* object-related actions (HMt and prehension)  
20 and the areas more specifically involved in the imitation of the observed *intransitive* action. The  
21 combination of these tasks within the same framework aims to investigate to which extent the  
22 intransitive praxis gestures, requiring the purposeful use of the hand for imitating meaningless or  
23 meaningful (communicative) gesture, exploit phylogenetically ancient parieto-frontal pathways  
24 subserving transitive object-oriented actions.

25

26

# 1 **Materials and methods**

## 2 **Patients' selection**

3 Enrolled in the study were 79 right-handed patients undergoing awake neurosurgery for a left-  
4 brain tumour resection (WHO Tumor grade: high-grade glioma (HGG) n=48, 61%; low-grade  
5 glioma (LGG) n= 27, 34%; others n= 4, 5%; Age: average =  $49.5 \pm 14.8$ , range 19 – 76; gender:  
6 69% male n=55, 64%; female n=24, 31%). All patients were assessed for handedness using the  
7 Edinburgh Handedness Inventory and underwent a pre-operative, 7-days and 1-month  
8 postoperative neuropsychological evaluation and objective neurological examinations. The  
9 seventy-nine patients were included meeting the following inclusion criteria:

- 10 1) first procedure of tumour resection, to minimize the impact of the disease and treatments on  
11 brain functional reorganization;
- 12 2) tumour not infiltrating the Supplementary motor area, the precentral/postcentral hand-knob in  
13 order avoid the inclusion of patients with invalidating basic motor and somatosensory  
14 impairments.
- 15 3) post-operative MRC (Medical Research Council) upper-limb score  $\geq 4$  in order to ensure the  
16 absence of elementary motor deficits affecting the praxis and prehension assessments.
- 17 4) post-operative absence of severe sensory (tactile and visual) deficit assessed by means of  
18 neurological assessment.
- 19 5) post-operative absence of language comprehension deficits impacting the reliability of the  
20 assessments.
- 21 6) pre-operative absence of pathological score for ideomotor apraxia (De Renzi global score  $> 53$ )
- 22 7) pre-operative absence of any clinically observable deficit during object prehension-  
23 manipulation (ARAT global score = 48)

24 According to tumor localization patients were categorized mainly as frontal/fronto-temporal  
25 (n=27, mean cavity volume:  $113.378 \pm 75.868$  voxels, range 3.607-259.376), parietal/parieto-  
26 temporal (n=34, mean cavity volume:  $48.528 \pm 32.429$  voxels, range 12.949-152.927), and  
27 temporal (n=18, mean cavity volume:  $61.679 \pm 38.321$  voxels, range: 13.952-135.001).

1 All participants gave written informed consent to the surgical mapping procedure (IRB1299) and  
2 data analysis for research purposes, following the principles outlined in the Declaration of  
3 Helsinki.

4

## 5 **Intraoperative mapping with hand-manipulation task and workflow** 6 **of the study**

7 All patients underwent the standard brain mapping for language<sup>27</sup>, motor<sup>28-31</sup>, executive  
8 functions<sup>32,33</sup>, visual field<sup>34</sup> and manipulation abilities<sup>20-24</sup>. Specifically, the areas crucial for  
9 manipulation abilities were assessed intraoperatively with a dedicated task, the Hand Manipulation  
10 Task (HMt, see Fig 1). During HMt, patient was asked to grasp and rotate continuously, with  
11 thumb and index opposition (precision grip), a specific manipulandum-shaped object. The HMt  
12 was performed in absence of visual guidance. During HMt execution, the surgeon stimulated with  
13 DES the cortical and subcortical areas required by the clinical needs. During task execution, the  
14 hand behavior and the intrinsic and extrinsic hand muscles' electrical activity (EMG) were  
15 recorded and synchronized with DES. Intraoperative distinction between brain sites where  
16 stimulation interfered (effective sites) or did not interfere (ineffective sites) with task execution  
17 was based on both visual inspection of hand behavior and the online monitoring of the EMG  
18 activity. An offline analysis of the EMG activity synchronized with video recordings of hand-  
19 movement was then performed, allowing a more refined quantitative analysis (for further details  
20 see<sup>21-24</sup>).

21 Aside to the intraoperative assessment, a peri-operative evaluation of patients was performed  
22 before, at 7 days (early phase) and at 1-month from the surgery by using an extensive  
23 neuropsychological evaluation<sup>35</sup> and specific tests to assess: A) elementary sensory and motor  
24 disorders (objective neurological evaluation), B) visuo-guided prehension (reaching-to-grasping)  
25 and C) praxis abilities (imitation of intransitive gestures).

26 The pre-operative assessment was needed to set the baseline condition of each patient (see  
27 inclusion criteria). The post-operative scores for prehension and praxis abilities of the selected  
28 patients were used in the Support Vector Regression Lesion Symptom Mapping (SVR-LSM)  
29 analysis to localize, among the brain areas surgically resected, those associated to lower scores in

1 prehension and praxis performances. These results were spatially matched with the probability  
2 maps reporting the main cortical and subcortical intraoperative sites where DES interfered with  
3 manipulation abilities. See Fig 1 for a resume of the methodological approach.

## 5 **Clinical Assessments**

### 6 **Prehension assessment**

7 The visually guided reaching-to-grasping abilities were assessed by using the ARAT (Action  
8 Research Arm Test) scale, which is composed of 18 items divided in four sub-scales: grasp, grip,  
9 pinch and gross movements<sup>36</sup>. For the specific purpose of the study, the items were performed with  
10 the right upper-limb (contralateral to the affected hemisphere). The ARAT was performed  
11 following a standardized protocol and scoring<sup>37</sup>. Instructions were read aloud and a visual  
12 demonstration for each item was provided. A time limit of 60 seconds was set to complete each  
13 task. The performance of each task was scored from 0 to 3: score = 3 was given when the task was  
14 performed correctly in < 5 seconds (behavioral criteria outlined by <sup>37</sup>); score = 2 when the task  
15 was completed with overt abnormal hand and/or arm movements or with delay (from 6 to 60  
16 seconds); score = 1 when the task was partially performed within the 60 seconds; score = 0 when  
17 none of the hand or arm movement required by the task was performed in 60 seconds. Relevant  
18 parameters adopted for the evaluation of the hand-arm performance of all sub items were: 1)  
19 smoothness and precision of the reaching movement toward the object-space and, 2) stability and  
20 congruency of the grip for each specific target. Since the focus of the ARAT, in the present study,  
21 was the clinical assessment of the visually guided reaching-to-grasping movements, the score  
22 obtained with gross movements was not included in the analysis, thus the maximum ARAT score  
23 (ARAT global score) was 48.

### 25 **Ideomotor Apraxia assessment**

26 Praxis abilities were assessed with De Renzi test<sup>38,39</sup>: patients were asked to imitate 24 intransitive  
27 gestures with the fingers, hand and arm. The task was performed with the contralesional right hand.  
28 During test, the patients were asked to maintain the same body posture adopted during the ARAT  
29 while the examiners, sitting in front, showed each item to be imitated. To ensure the full



1 understanding of the instructions by the patients, the assessment started with a simple, test-  
2 unrelated, gesture to be imitated (rise the hand). Each gesture was presented up to three times and  
3 the performance scored from 3 to 0 depending on whether the execution was correct the first,  
4 second, third attempt or never. Among the 24 items, 12 were symbolic (meaningful) and 12 non-  
5 symbolic (meaningless) gestures. The total score was 72 (De Renzi global score). Notably, the  
6 imitation of the intransitive gesture relies on visual, proprioceptive and tactile feedback provided  
7 by contact between different fingers, between the hand/fingers and another body part or another  
8 external surface (see some examples in Fig 1). In this regard, the tactile feedback is crucial for the  
9 correct execution of the gesture and its monitoring as well as for the correct object-grip during the  
10 visuo-guided prehension (ARAT).

11

## 12 **Image acquisition and lesion analysis**

13 As part of the clinical routine, pre- and postoperative MRI was performed on a Philips Intera 3 T  
14 scanner (Koninklijke Philips N.V.) and acquired for lesion morphological characterization and  
15 volumetric assessment<sup>28</sup>. A post-contrast gadolinium T1-MPRAGE sequence was performed using  
16 the following parameters TE: 2.75 ms, TR: 1600 ms, flip angle 9°, IT 900 ms; 176 slices; isotropic  
17 voxel size of 1 mm.

18

## 19 **Resection cavity tracing and Spatial Normalization**

20 For each patient, the resection cavity was manually drawn on the post-operative volumetric T1-  
21 weighted images acquired at 5/7 days after surgery by L.F. with MRIcron software<sup>40</sup>. This  
22 approach, with respect to the follow-up MRI (>1 month), had the benefit to avoid interference with  
23 adjuvant treatments and it is closest in time to the early post-operative praxis/prehension  
24 evaluation. Post-operative T1 and cavities of the patients were normalized to 1x1x1mm resolution  
25 to Montreal Neurological Institute (MNI) space using the Clinical Toolbox implemented in SPM  
26 12. In all patients, the normalization procedure was applied by using the enantiomorphic algorithm  
27 and lesion masking procedure. Since the study was based on performance assessments in early  
28 postoperative phase the cavity estimation was smoothed (FWHM 3 mm, Threshold 0.05) for  
29 including a small amount of surrounding tissue. The rationale was that the tissue surrounding the  
30 resection cavity, spared from the resection, during the early post-operative phase undergoes

1 inflammation that transiently impairs its functions possibly affecting the behavioral performance.  
2 In addition, for each patient we also estimated in the post-operative DWI MRI sequence the  
3 occurrence of ischemic lesions, in order to exclude patients with post-operative vascular diseases.  
4 Following the normalization procedure, for each patient the results were checked with CheckReg  
5 function in SPM 12.

## 7 **Lesion–Symptom Mapping**

8 Multivariate Lesion symptom mapping has been performed by using support vector regression-  
9 LSM (SVR-LSM<sup>41</sup>) implemented by DeMarco and Turkeltaub in a MATLAB-based toolbox<sup>42</sup>.  
10 The analysis was performed by applying functionalities of the Statistic and Machine Learning  
11 Toolbox within MATLAB 2019b. Optimization of hyperparameters was performed via  
12 resubstitution loss and Bayesian optimization with 200 iterations and 5-fold cross-validation, as  
13 implemented in Matlab (bayesopt) and recently applied by the authors of the MatLab-base  
14 software and others group<sup>44–46</sup>. In addition, the range for the optimized parameters was set  
15 following the range of C and Gamma suggested by Zhang et al.<sup>41</sup> and more recently adopted by  
16 Wiesen et al.<sup>43</sup>. C range = 1-80, Gamma equivalent Sigma range = 0.1-30 (conversion was  
17 performed by using *function=gamma2sigma* available in SVR-LSM gui). A default Epsilon range  
18 was set. For each analysis and combination of parameters selected after optimization procedure,  
19 both prediction accuracy and reproducibility were evaluated. Based on other studies using similar  
20 procedure<sup>44,45</sup>, we considered reliable the LSM results when showing accuracy  $\geq 0.25$  and  
21 reproducibility  $\geq 0.85$ .

22 SVR-LSM was used to identify in the early post-operative phase significant voxels included in the  
23 resection cavities and/or around the borders associated with lower scores in the visuo-guided  
24 prehension (ARAT) and imitation of intransitive gestures (De Renzi) performance. Large lesions  
25 often result in more severe behavioral impairments, regardless of location, decreasing the  
26 specificity of the results. Thus, in the present study this aspect was controlled by applying the  
27 direct Total Lesion Volume Control (dTLVC) as implemented by Zhang et al.<sup>41</sup>. The resulting  
28 SVR- $\beta$  values were thresholded at  $p < .005$  and corrected with cluster size at  $p < .05$  both based  
29 on 5000 permutations. In addition, continuous permutation-based family wise error (CFWE)  
30 correction was configured to permit 1.0 mm<sup>3</sup> of false positives (desired  $v = 1$  whole voxels) and  
31 accept a family-wise error rate (FWER) of 0.05.

## 1 **Matching the SVR-LSM results (praxis and prehension) and intraoperative** 2 **DES (Hmt)**

3

### 4 **Anatomical reconstruction of intraoperative DES results.**

5 In order to match the post-operative SVR-LSM clusters associated to prehension and praxis lower  
6 scores with intraoperative cortical and white matter manipulation sites, the anatomical localization  
7 of each intraoperative effective site in each patient was needed.

8 **Cortical sites:** the exact position of the sites was reported on the 3D MRI (pre-operative) cortical  
9 surface of each patient reconstructed with FreeSurfer by means of Brainstorm<sup>46</sup> under the guidance  
10 of the flap-video and intraoperative coordinates from neuronavigation (BrainLab). Subsequently  
11 the MRI and site were co-registered to MNI space using Brainstorm and clinical toolbox in SPM  
12 12.

13 **Subcortical white matter sites:** included in this analysis were the effective stimulated sites  
14 located in the white matter below the sulci and/or gray matter as reported by intraoperative  
15 coordinates in native space and surgical flap. During postoperative reconstruction, the site was  
16 drawn on the preoperative axial volumetric T1 as spherical ROI (6mm diameter, similar to the  
17 resolution of the bipolar probe) based on image and related native coordinates acquired with  
18 neuronavigation system. The localization of the site was also verified using as reference the  
19 postoperative T1. Being the effective sites used as functional borders to stop the resection, the edge  
20 of the resection cavity represents an optimal landmark to confirm the site positioning. To this aim,  
21 in each patient, the stimulation sites, the preoperative T1 and the postoperative T1 were co-  
22 registered to the MNI space by means of the Clinical Toolbox implemented in SPM12.

23 The accuracy of each co-registration was visually confirmed using the SPM12 CheckReg function.  
24 Finally, the anatomical localization of each site in each patient was confirmed by the first operating  
25 surgeon (L.B.).

26 To investigate whether the effective sites clustered in specific subsectors, a modified in-house  
27 version of probability kernel density estimation (PDE analysis) implemented in MatLab was  
28 applied (see<sup>21,22</sup> for details regarding PDE for cortical sites and<sup>24</sup> for PDE for subcortical sites).

29

## 1 **Results**

2 In all the enrolled patients the impact of basic (primary) motor disorders in performance of the  
3 ARAT and De Renzi tests, was excluded by enrolling patients with MRC score  $> 4$  and with score  
4 = 3 in grasping the “heaviest” wooden cube (10 cm) of the ARAT. The level of whole handgrip  
5 strength and somatosensory feedback needed to execute the task excludes the occurrence of  
6 primary somatosensory and motor deficits possibly affecting ARAT and De Renzi tasks. Based on  
7 these criteria, 7 patients initially recruited were not included in the final analysis.

8 Results will report: A) ARAT and De Renzi clinical scores distribution; B) SVR-LSM results; C)  
9 intraoperative DES results; D) Spatial matching between SVR-LSM and DES.

10

### 11 **ARAT and De Renzi clinical scores**

12 **ARAT.** Since ARAT scores are a continuous measure, without categorical cutoff scores, patients  
13 were ranked based on the number of items showing a performance decrease with respect to the  
14 pre-operative assessment. **Pre-operative phase:** none of the patients showed observable deficits.

15 **Early post-operative:** 19 out of 79 patients reported a lower score in the early post-operative  
16 phase subdivided as follows: A) 10 out of 79 patients with a score decrease only in the pinch  
17 subscale (12.6% of patients, average global score 45.2, range 38-46); B) 5 out of 79 patients with  
18 a score decrease in pinch-grip items (6.3% of patients, average global score 38.2, range 33-42); C)  
19 4 patients with a score decrease in grasp-grip-pinch (5% of patients, average global score 27.25,  
20 range 20-35). **Post-operative 1 month:** at population level, the ARAT global score significantly  
21 improved compared to the early post-operative phase with no significant difference with the pre-  
22 operative phase (Fig 2B: ARAT scores distribution and statistics).

23 **De Renzi. Pre-operative phase:** none of the included patients had a pathological score and only  
24 3 patients showed a borderline global score. **Early post-operative:** 11 out of 79 patients global  
25 score fell below the cut-off (13.9% of the patients, cut off  $< 53$ , average 41.5, range 30-51) while  
26 6 patients were borderline (7.6%, cut off 53-62, average 59.2, range 53-62). The remaining 62  
27 patients scored above the cut-off (78.5%, average 70.9, range 63-72). **Post-operative 1 month:** at  
28 population level, De Renzi global score significantly improved compared to the early post-

1 operative phase with no significant difference with the pre-operative phase. These results, coherent  
2 with previous study of our group<sup>20</sup>, confirm the transitory nature of the early post-operative  
3 outcome (Fig 2C: De Renzi scores distribution and statistics).

4 See Supplementary Table 1 for clinical details.

5

6 **De Renzi and ARAT scores correlation.** To assess whether the De Renzi and ARAT early  
7 post-operative scores are correlated, a Spearman correlation was performed on the global scores.  
8 At population level ARAT and De Renzi global scores significantly correlated (Spearman  
9 correlation  $r=0.557$ ,  $p<.05$ ). However, among ARAT items, the regression analysis showed that  
10 only score of the pinch item significantly predicted a decline in the De Renzi performance  
11 (predictors: grasp, grip, pinch; dependent variable: De Renzi global score;  $F(3,75)=9.74$ ,  $p<.000$ ,  
12  $R^2_{\text{adjusted}}=0.25$ ; grasp  $F=1.72$ ,  $p=0.19$ ,  $\beta=-0.22$ ; grip  $F=2.3$ ,  $p=0.13$ ,  $\beta=0.306$ ; pinch  $F=6.17$ ,  
13  $p=0.015$ ,  $\beta=0.408$ ).

14

## 15 **SVR-LSM results**

### 16 **Localization of surgical cavities**

17 The SVR-LSM analysis was restricted to the minimum overlap of 7 patients (about 9% of the  
18 whole sample). The minimum overlap involved the frontal areas (excluding BA4-BA6), parietal  
19 lobe (excluding area 3a, 3b, 1 and marginally including area 2), the temporal lobe, the insular  
20 cortex and adjacent opercular regions (Fig 2A). Due to the significant correlation between  
21 prehension and praxis global scores, we performed SVR-LSM analysis with and without covariate  
22 in order to investigate specific (covariates results) and common (overlap of non-covariate results)  
23 voxels for prehension and praxis. SVR-LSM analysis was performed for both early post-operative  
24 and 1-month De Renzi and ARAT scores. We report only the early post-operative results, since  
25 the prediction accuracy and reproducibility values for the SVR-LSM at 1-month fell below the  
26 threshold considered (accuracy  $< 0.25$ , reproducibility  $< 0.85$ ).

27 **Prehension abilities (De Renzi covariate).** Results showed that a decrease in the visuo-  
28 guided object-prehension abilities was associated to CFWER cluster involving: 1) the superior

1 parietal lobe (7AL, 7PC, 5L and LIP) and 2) the precuneus (31pd) (Fig 3A-C). Hyperparameters:  
2 Cost/Box Constraint = 77, Sigma/Kernel scale = 1.54, Epsilon = 1.9; Prediction accuracy = 0.41,  
3 reproducibility index  $r = 0.86$ .

4 **Praxis abilities (ARAT global score covariate).** Results showed that a decrease in the  
5 imitation of intransitive gesture was associated to a CFWER cluster involving: 1) the intraparietal  
6 (AIP, IP2) and 2) the inferior parietal lobe (PF/PFm) (Fig 3B-C). Hyperparameters: Cost/Box  
7 Constraint = 75, Sigma/Kernel scale = 1.25, Epsilon = 0.1; Prediction accuracy = 0.54,  
8 reproducibility index  $r = 0.86$ .

9 **Meaningful vs Meaningless praxis gestures (ARAT global score covariate).**  
10 Results showed that although the two CFWER clusters overlapped within the intraparietal sulcus  
11 (IPS), meaningful gesture clustered in a wider area in the inferior parietal lobe (IPL) with respect  
12 to meaningless gesture, including mainly PF (Fig 3B). Hyperparameters Meaningful: Cost/Box  
13 Constraint = 79, Sigma/Kernel scale = 1.29, Epsilon = 1.8; Prediction accuracy = 0.53,  
14 reproducibility index  $r = 0.87$ . Hyperparameters Meaningless: Cost/Box Constraint = 79,  
15 Sigma/Kernel scale = 1.13, Epsilon = 2.49; Prediction accuracy = 0.48, reproducibility index  $r =$   
16  $0.85$ .

17 **Common region (overlap between ARAT and De Renzi not covariate results).**  
18 Results showed that common voxels were found mainly within the dorsal bank of the intraparietal  
19 sulcus and adjacent dorsal postcentral sulcus (Fig. 3D). Hyperparameters ARAT: Cost/Box  
20 Constraint = 30.6, Sigma/Kernel scale = 1, Epsilon = 0.1; Prediction accuracy = 0.45,  
21 reproducibility index  $r = 0.85$ . Hyperparameters De Renzi: Cost/Box Constraint = 45.3,  
22 Sigma/Kernel scale = 1.23, Epsilon = 0.38; Prediction accuracy = 0.59, reproducibility index  $r =$   
23  $0.86$ .

## 24 25 **Intraoperative DES results.**

26 Previous studies of our group reported evidence that intraoperative DES delivered on specific  
27 premotor<sup>21</sup> and parietal areas<sup>22</sup> as well as on frontal white matter<sup>24</sup> affects the performance of tasks  
28 requiring hand-object manipulation (HMt). Since the SVR-LSM analysis performed in the present

1 study highlighted significant clusters only in the parietal lobe, the spatial matching analysis  
2 between lesion results and intraoperative DES results was constrained to the intraoperative data  
3 recorded within the parietal lobe<sup>22</sup> at cortical and, as novel finding here, at subcortical level within  
4 the parietal white matter. Cortical and subcortical data together allow a more comprehensive  
5 spatial matching with SVR-LSM results.

6  
7 **Cortical results.** These results were previously published<sup>21</sup>. In brief, intraoperative DES of  
8 specific parietal sectors interfered with performance of HMt by disrupting the hand-muscles'  
9 recruitment. Probability density estimation, obtained by contrasting effective sites (n=111) with  
10 ineffective sites, highlighted significant responsive clusters in the post-central gyrus  
11 (somatosensory fingers representation), the putative human homologue of monkey AIP (phAIP<sup>47</sup>)  
12 and, more marginally, the anterior PF/PFt within the IPL. (Fig 4A and B(i-ii)). Within the posterior  
13 parietal cortex, DES effect on HMt ranged from an abrupt arrest (task-arrest) mainly reported  
14 within phAIP, to a lack of finger coordination (task-clumsy) mainly reported within anterior IPL  
15 (PF), both associated to different degree of muscle suppression (Fig 4B(iii)).

16 **White matter results.** Considering the 8 patients showing effective sites in the deep white  
17 matter of the posterior parietal cortex, 16 effective sites were localized (according to the patient  
18 native space) in the white matter below the fundus of rostral IPS and postcentral sulcus, broadly  
19 corresponding to the white matter below phAIP and PF/PFt. Task-arrest (n=7) responses were  
20 mainly found below AIP while task-clumsy (n=9) were adjacent to the white matter below PF (Fig  
21 4C(i)), coherently with cortical distribution.

22  
23 **Matching praxis and manipulation cortical and subcortical sites.** The spatial  
24 matching analysis showed that intraoperative manipulation-sites and praxis-related clusters co-  
25 localized within rostral IPS and IPL regions. More specifically:

26 1) Within rostral IPS, the intraoperative manipulation-sites clustered within the anterior part of  
27 phAIP, while praxis-related voxels at the transition between phAIP and dorso-anterior intraparietal  
28 sulcus (DIPSA) (Fig 4B(i-ii)).

1 2) Within the rostral IPL, despite the lower level of probability, intraoperative manipulation-sites  
2 clustered in anterior PF, while praxis-related voxels at the transition between PF and PFm (Fig  
3 4B(i-ii)).

4 3) The matching obtained at cortical level was specular at subcortical level (Fig. 4C(i-ii)).

5 4) The anterior IPS was associated to both meaningless and meaningful gestures, while anterior  
6 IPL was associated to meaningful gestures. Parallel to this distinction, the manipulation-sites  
7 within rostral IPS (phAIP) and IPL (PF) showed different features of motor impairment induced  
8 by DES during HMt, task-arrest and clumsy respectively (Fig. 4B(iii-iiii) and 4C(i)).

## 9 **Discussion**

10 In the present study, we used complementary causal techniques in brain tumor patients: the post-  
11 operative lesion mapping to investigate prehension and praxis-related regions, and the  
12 intraoperative direct electrical stimulation to investigate object manipulation-related regions. A  
13 spatial matching between the results of the two techniques was employed in order to investigate  
14 the anatomo-functional relationship between the neural substrates subserving praxis abilities  
15 (imitation of intransitive gestures) and the phylogenetically old *building blocks* subserving object-  
16 oriented actions (prehension and object-manipulation).

17 Studies in stroke patients significantly contributed to outline the current theoretical, anatomical  
18 and clinical framework in the field of praxis-related disorders. However, several aspects related to  
19 the different etiology and clinical outcome prevent a strict comparison between LSM results  
20 collected in stroke and brain tumor patients<sup>48</sup>. In this regard, brain tumor is a focal lesion and the  
21 resulting resection cavity following the brain mapping technique is *well-identifiable* and  
22 *functionally* delimited.

23 In a different frame, also fMRI studies provided important insight in the field of praxis movements.  
24 However, fMRI data are correlational by nature and do not allow to investigate the causal  
25 functional role of the different nodes belonging to the PRN. In this regard, the LSM and DES are  
26 historically considered the gold standard for causal mapping of human brain functions allowing to  
27 draw causal inferences about the role of a specific region with respect to the investigated function,  
28 a crucial aspect for translating knowledge into therapeutic targets<sup>49</sup>.



1 However, despite the aforementioned advantages, both LSM and DES have limitations in the  
2 present clinical context, in particular the pre-operative brain functional reorganization and the  
3 morphological displacement due to tumor mass. Our group adopts specific patients' inclusion  
4 criteria for reducing the impact of tumor displacement<sup>22</sup> and for estimating the quality of the  
5 coregistration<sup>24</sup>. Despite these criteria cannot fully prevent the impact of such variables on results,  
6 the spatial matching between the intraoperative DES and post-operative LSM results is in line with  
7 the clinical aim of the intraoperative brain mapping, supporting a good reliability of the results  
8 obtained by integrating different methods, at least within the sample of patients enrolled in this  
9 study. Finally, based on recent guidelines<sup>50</sup>, another potential limitation of the present study is the  
10 low sample of patients required to optimally model voxel-wise lesion location in SVR-LSM.  
11 However, considering that brain tumor is a rare pathology and the patients' inclusion criteria  
12 adopted for the aim of the present study, the resection cavities equally covered frontal, parietal and  
13 temporal areas, allowing to causally test the main nodes of the dorso-dorsal and dorso-ventral  
14 pathways.

15

## 16 **The dorso-ventral stream is specifically implicated in praxis abilities**

17 The first result emerging from this study was the higher relevance of the left posterior parietal  
18 lobe, with respect to prefrontal or temporal, in the onset of ideomotor apraxia, in agreement with  
19 very first observations<sup>51</sup>. Within the parietal lobe, neuroimaging and lesion studies provided  
20 evidence of the involvement of several dorso-dorsal and dorso-ventral parietal sectors in imitation  
21 of intransitive gestures<sup>52</sup>. The present study, investigating ideomotor apraxia by using prehension  
22 performance as covariate, clearly showed that specific ideomotor praxis deficits were associated  
23 to parietal sectors included in the dorso-ventral stream rather than in the dorso-dorsal one.  
24 Specifically, the borders of resections adjacent to rostral IPS and IPL are associated to a transient  
25 impairment in imitation of intransitive gestures, while more dorsal resections involving the anterior  
26 SPL and the precuneus cause a specific impairment in visually guided object-prehension. Notably,  
27 the absence of a quantitative kinematic-based approach to prehension movements prevent, in the  
28 present study, the investigation of micro-features of movement. However, coherently with our  
29 finding, these areas are classically associated to optic ataxia, a high order deficit in reaching visual  
30 goals, hand pre-shaping and on-line correction during reaching<sup>53-55</sup>.

1 The dissociation found in the present study is in agreement with evidence suggesting that, although  
2 highly coordinated, dorso-dorsal and dorso-ventral pathways play distinct roles in hand actions. In  
3 this regard, converging evidence has shown that the dorso-dorsal system, also called *Grasp system*,  
4 processes visual-related object physical features for the purpose of prehensile action, while the  
5 dorso-ventral stream, also called *Use system*, is involved in the long-term storage of the particular  
6 skilled actions associated with familiar objects<sup>56</sup>. Coherently, the two systems are differently  
7 connected with temporal (ventral stream) areas and are involved in the extraction of different type  
8 of object affordances. Accordingly, the invariant object features, i.e. *stable affordances*, emerge  
9 from the slow “offline” processing of the visual information based on memorized object  
10 knowledge taken over by the dorso-ventral pathway. Differently, changing or temporary object  
11 physical features, i.e. *variable affordances*, emerge from the fast online processing of visual  
12 information during actual object interaction mainly in charge to the dorso-dorsal pathway<sup>57</sup>. The  
13 present results may extend these distinctions showing that specific parietal nodes within the dorso-  
14 ventral pathway are crucial also for imitation of intransitive gestures. In this regard, the gesture  
15 execution occurs through its observation and recently it has been proposed that visual encoding of  
16 other’s actions, i.e. *social affordances* -conceived as the variety of action possibilities offered to  
17 an individual by other agent’s behavior-, exist alongside object affordances. This hypothesis  
18 extends the concept of affordances from inanimate object to the other’s action<sup>58</sup>. In line with this  
19 view, the present results may suggest that dorso-ventral pathway not only encodes stable  
20 (complex) affordances related to purposeful interaction with objects, but may extract also social  
21 affordances via the observation of the gesture to be imitated. The latter mechanism may be crucial  
22 in ideomotor apraxia, possibly favoring the visuomotor conversion of the observed gesture.

23 Furthermore, although the two streams process distinct action features, the IPS emerge as  
24 convergence zone<sup>57</sup>. This finding is coherent with the results of the present study, which points to  
25 the dorsal bank of the IPS, mainly corresponding to the transition between dorso-anterior and  
26 posterior intraparietal sulcus (DIPSA and DIPSM), as a potential common region. This fits with  
27 the positive correlation found between prehension and praxis scores, which suggested that to some  
28 extent the two pathways work along a functional continuum rather than in dichotomous way. In  
29 this regard, the existence of this intraparietal hub, may subserve common functional aspects and/or  
30 the exchange of information between dorso-dorsal and dorso-ventral streams<sup>57</sup>, possibly  
31 contributing at the extremely flexible use of our hand sensorimotor repertoire, from concrete action

1 specification to abstract action goals<sup>59</sup>. Interestingly, the regression analysis showed that the sole  
2 ARAT item significantly predicting the De Renzi performance was the pinch. The pinch item  
3 requires a higher level of dexterity with respect to the other ARAT items and often requires an  
4 “unusual” or “less functional” grip posture (i.e. to execute a precision grasping with thumb-  
5 ring/thumb-middle finger opposition). Although the interpretation of this result is challenging, it  
6 might suggest that, when the required hand-action is less consolidated in our daily sensorimotor  
7 repertoire, an efficient communication between streams via intraparietal hubs could be crucial for  
8 its implementation.

9

## 10 **Parietal lobe hosts distinct praxis route and sensorimotor processes:** 11 **a comparative perspective**

12 As previously reported<sup>22</sup>, DES delivered during HMT onto phAIP evoked an abrupt arrest (task-  
13 arrest) while on PF evoked a loss of finger’s coordination (i.e. task-clumsy). We suggested that  
14 the task arrest might reflect the “transient impairment” of a parietal sector shaping, with a relatively  
15 direct access, the motor output. Differently, the clumsy pattern might reflect the “transient  
16 impairment” of a parietal sector hierarchically far with respect to the cortical motor output. Overall,  
17 we suggest that the different impairments may ultimately arise from a different role of rostral IPS  
18 and IPL regions in shaping hand-motor output.

19 Paralleling the anatomical distribution of the different effects of DES on HMT, the LSM results  
20 showed that the parietal sectors adjacent to phAIP and PF were associated to different deficits in  
21 imitation/execution of gestures. Resections involving the rostral IPS affected the imitation of both  
22 meaningless and meaningful gestures (no gesture type selectivity), while resections involving the  
23 rostral PF complex affected mainly the imitation of meaningful gestures (gesture type selectivity),  
24 in line with the evidence of a dissociation between the two types of intransitive gestures<sup>60,61</sup>.  
25 Taking together, the co-localization between intraoperative DES and LSM results suggests that the  
26 different motor impairments evoked by DES within phAIP and PF may reflect different  
27 sensorimotor process, possibly subserving different pathways for gesture imitation. In this regard,  
28 gesture imitation is indeed subserved by two pathways: the *direct* pathway involved in the  
29 execution of the observed gesture regardless to its content; the *indirect* pathway controlling

1 gestures reproduction through the access to their meaning in the semantic memory<sup>62</sup>. In this light,  
2 our results suggest that the former may take place within rostral IPS (cortical area hosting task-  
3 arrest and no gesture type selectivity), while the latter within the PF complex (cortical area hosting  
4 task-clumsy and gesture type selectivity).

## 6 **The rostral intraparietal sulcus and the direct pathway**

7 The co-localization within rostral IPS of DES-related effects on manipulation (the arrest effect)  
8 and voxel associated to imitation of the observed gestures (no gesture type specificity) might  
9 suggest that the integrity of this region could be crucial for both the motor implementation and the  
10 visuomotor conversion of the observed gesture.

11 In this regard, recently has been shown that monkeys and human rostral IPS hosts neurons selective  
12 for observed manipulative actions claimed to support a stable read out of the observed actions  
13 across visual formats<sup>58,63–65</sup>. Despite the impressive similarities between human and monkey  
14 results, neurons in humans showed a greater invariance and generalization across viewpoint  
15 compared to monkey, including responses to reading action verbs. The human's greater invariance  
16 and generalization may reasonably point to the human IPS as the encoder of a wide variety of  
17 actions formats, including non-manipulative actions such as the processing of the observed  
18 intransitive gesture. This hypothesis is coherent with fMRI studies in healthy subjects, showing  
19 that both transitive and intransitive gestures are processed within the left-lateralized praxis  
20 representation network, including the rostral IPS<sup>10,66,67</sup>. The selectivity for the observed  
21 manipulative actions within the rostral IPS, essential for action planning during social interaction  
22 and interindividual coordination, is suggested to work in parallel with the neural population  
23 involved in the sensorimotor transformation for object-oriented action<sup>58</sup>. Based on this premise we  
24 may hypothesize that praxis-significant voxels within phAIP/DIPSA transition, could reflect the  
25 role of this sector in the visual processing of the observed gesture. Moreover, since the DES of  
26 rostral phAIP affected the hand-manipulation motor output evoking task-arrest responses, we  
27 might speculate that visual information of the observed gesture might be exploited by phAIP and  
28 its connectivity with premotor areas for the motor implementation of the gesture itself. This

1 functional organization fits with the supposed role of phAIP and DIPSA as motor and visual sector  
2 of monkey AIP respectively<sup>47</sup>.

3 Despite obtained by the complementary use of different tasks (HMt and De Renzi) testing distinct  
4 action features (transitive vs intransitive), these results could be coherent with the idea of a direct  
5 pathway within the rostral IPS subserving visuo-motor conversion during gestures  
6 observation/imitation. Notably, this pathway seems to rely prevalently on phylogenetically old  
7 rostral IPS nodes, with its main hub within phAIP, a core area belonging to the *lateral grasping*  
8 *network* originally described in monkey (LGN<sup>3</sup>). The LGN belongs to the dorso-ventral pathway  
9 and is considered a cognitive interface for hand actions<sup>4</sup>. Our finding about the co-localization of  
10 manipulation and praxis voxels within the human rostral IPS strengthens the hypothesis that the  
11 anatomo-functional features of the monkey's LGN fostered the cognitive upgrade of the dorso-  
12 ventral pathway further subserving the unique human praxis repertoire. Moreover, the dual role in  
13 hand-object and hand-gesture oriented actions could reasonably explain why the preservation of  
14 the rostral IPS during intraoperative mapping with the HMt, a task actually not assessing directly  
15 praxis functions, resulted in prevention of permanent ideomotor apraxia symptoms.

16

## 17 **The inferior parietal lobe and the indirect pathway**

18 Conversely, according to LSM results, lesions within PF complex impairs critically imitation of  
19 meaningful gestures, pointing at this region, with access to semantic knowledge, as a key structure  
20 in the indirect pathway for gesture imitation. Interestingly, DES of PF and its surrounding white  
21 matter alters motor execution by evoking task-clumsy responses, hypothesized to reflect a remote  
22 access to the motor output with respect to task-arrest. In light of this evidence, we may speculate  
23 that the properties of the parietal clumsy region, PF complex, might subserve the integration and  
24 gating of conceptual and semantic knowledge into the pragmatic sensorimotor workflow. This  
25 hypothesis is in agreement with theories suggesting that meaning or conceptual knowledge would  
26 emerge from interactions between multimodal areas and the pathways processing motor  
27 information<sup>68</sup>. Rostral PF complex might favor this connection. In this frame, the overall IPL is  
28 considered a semantic hub active during semantic processing of cross-modal spatial and temporal  
29 configurations<sup>69</sup>, thus we hypothesize that PF-related pathways may act as passageway integrating

1 this information from parietal and temporal high-order multimodal areas, into the sensorimotor  
2 workflow taken over by rostral IPS.

3

## 4 **Conclusion**

5 Overall, the anatomo-functional interaction between rostral IPS and IPL areas likely represents the  
6 neural mechanism by which cognition shapes sensorimotor processing ultimately promoting the  
7 unique human hand actions repertoire.

8 From a clinical perspective, our results suggest that the preservation of this mechanism is crucial  
9 for avoiding long standing ideomotor apraxia in brain tumor patients. Preservation of these dorso-  
10 ventral parietal regions was possible thanks to the DES applied during HMt, which allowed to  
11 identify the functional borders of these areas at cortical and subcortical level, as clearly showed by  
12 the spatial matching between DES and LSM results. Therefore, the transient nature of the symptom  
13 may be due to the inflammatory state of the tissues preserved at the edge of the resection and/or to  
14 a partial impairment of its functioning. Regarding the latter point we could not exclude that, since  
15 their role as hub regions within the PRN, these areas might host an extended connectivity, which  
16 may promote functional compensatory mechanisms<sup>70</sup>.

17 To summarize, the present results showed a functional dissociation between dorso-dorsal and  
18 dorso-ventral streams and within the dorso-ventral one. First, it emerged the existence of a parietal  
19 dorso-lateral functional continuum subserving the transition from transitive object-oriented actions  
20 (dorso-dorsal pathway) to intransitive praxis gestures (dorso-ventral pathway), with specific  
21 rostral IPS sectors possibly working as convergent zone and regulating the flow of information  
22 between streams. Moreover, within the dorso-ventral stream our results showed a further  
23 dissociation between the role played by rostral IPS (mainly phAIP/DIPSA) and rostral IPL (mainly  
24 PF) in the type of gesture to be imitated (meaningless vs meaningful), to same extent mirroring  
25 the anatomo-functional distinction between object-manipulation and object(tool)-use<sup>5,71</sup>. Notably,  
26 the DES applied to these parietal regions evoked different type of motor impairments during the  
27 HMt execution, furthermore suggesting that these sectors may subserve distinct pathways for  
28 gesture imitation (direct vs indirect) via different hand-related somatomotor process.

1 Finally, these areas in addition to be part of the PRN and the LGN respectively in human and non-  
2 human primates, in particular IP2 and PFM areas are also core regions within the multiple demand  
3 network (MDN<sup>72</sup>). Since its definition, the MDN is implicated in a range of cognitively demanding  
4 tasks and appear central to intelligent action<sup>73</sup>. Taking together, this evidence highlights the  
5 multidimensional nature of the human praxis abilities and the importance of sensorimotor  
6 substrates adjacent and/or interleaved with multimodal areas in translating both gesture-related  
7 visual information and conceptual knowledge into a coherent motor representation.

8 Regarding limitations, a potential bias for the present results could be the lack of systematic control  
9 conditions allowing to quantify the integrity of the various modalities of sensory feedbacks  
10 exploited by the tasks, in order to exclude them as confounding factor. This is a relevant issue,  
11 since intraoperative HMT and postoperative tasks rely on sensory-guided modalities not completely  
12 overlapping. In this regard, this bias was qualitatively overcome by excluding patients that showed  
13 clinically overt basic visual and tactile deficits during neurological assessment. However, this  
14 procedure might be not exhaustive since the posterior parietal lobe hosts high-order sensory  
15 modalities crucial for the sensorimotor guidance of the three tasks. To reduce as possible also this  
16 confounding aspect, we used the ARAT score as covariate in LSM analysis for praxis functions.  
17 Since the ARAT execution rely on both somatosensory (shared with the HMT and praxis tasks) and  
18 visual-guidance (shared only with the praxis tasks), its use as covariate for investigating praxis  
19 abilities allow to isolate task-specific voxels for the imitation of the observed gesture. Finally,  
20 these methodological aspects allowed a spatial matching between ARAT vs De Renzi and HMT vs  
21 De Renzi mainly reflecting intrinsic tasks features.

## 23 **Data availability**

24 The data that support the findings of this study is available from the corresponding author, upon  
25 reasonable request.

26

## 1 **Funding**

2 This work has been supported by a grant from Associazione Italiana per la Ricerca sul Cancro  
3 (AIRC) to L.B.

## 4 **Competing interests**

5 The authors have no conflicting interests to report.

## 7 **Supplementary material**

8 Supplementary material is available at *Brain* online.

## 9 **References**

- 10 1. Jean AA. Developmental Dyspraxia and Adult Onset Apraxia Paperback ISBN-10.
- 11 2. Goldenberg G. Apraxia - the cognitive side of motor control. *Cortex*. 2014;57:270-274.
- 12 3. Borra E, Gerbella M, Rozzi S, Luppino G. The macaque lateral grasping network: A neural  
13 substrate for generating purposeful hand actions. *Neurosci Biobehav Rev*. 2017;75:65-90.
- 14 4. Borra E, Luppino G. Large-scale temporo-parieto-frontal networks for motor and cognitive  
15 motor functions in the primate brain. *Cortex*. 2019;118:19-37.
- 16 5. Orban GA, Caruana F. The neural basis of human tool use. *Front Psychol*. 2014;5(310).  
17 doi:10.3389/fpsyg.2014.00310.
- 18 6. Grafton ST. The cognitive neuroscience of prehension: recent developments. *Exp Brain Res*.  
19 2010;204(4):475-491. doi:10.1007/s00221-010-2315-2
- 20 7. Caminiti R, Innocenti GM, Battaglia-Mayer A. Organization and evolution of parieto-frontal  
21 processing streams in macaque monkeys and humans. *Neurosci Biobehav Rev*. 2015;56:73-  
22 96.



- 1 8. DC E, C D, DL D, MF G. Parcellations and Connectivity Patterns in Human and Macaque  
2 Cerebral Cortex. In: Kennedy H, Essen DC, Christen Y, eds. *Micro-, Meso- and Macro-*  
3 *Connectomics of the Brain*. Springer; 2016.
- 4 9. Frey SH. Tool use, communicative gesture and cerebral asymmetries in the modern human  
5 brain. *Philos Trans R Soc Lond B Biol Sci*. 2008;363(1499):1951-1957.  
6 doi:10.1098/rstb.2008.0008
- 7 10. Króliczak G, Frey SH. A common network in the left cerebral hemisphere represents planning  
8 of tool use pantomimes and familiar intransitive gestures at the hand-independent level. *Cereb*  
9 *Cortex*. 2009;19(10):2396-2410.
- 10 11. Przybylski Ł, Króliczak G. Planning Functional Grasps of Simple Tools Invokes the Hand-  
11 independent Praxis Representation Network: An fMRI Study. *J Int Neuropsychol Soc*.  
12 2017;Feb;23(2):108-120. doi:10.1017/S1355617716001120.
- 13 12. Buxbaum LJ, Shapiro AD, Coslett HB. Critical brain regions for tool-related and imitative  
14 actions: a componential analysis. *Brain*. 2014;137(Pt 7):1971-1985.  
15 doi:10.1093/brain/awu111
- 16 13. Hoeren M, Kümmerer D, Bormann T. Neural bases of imitation and pantomime in acute stroke  
17 patients: distinct streams for praxis. *Brain*. 2014;137(Pt 10):2796-2810.  
18 doi:10.1093/brain/awu203
- 19 14. Husain M. Neural control of hand movement. *Brain*. 2022;145(4):1191-1192.  
20 doi:10.1093/brain/awac095
- 21 15. Dressing A, Nitschke K, Kümmerer D. Distinct Contributions of Dorsal and Ventral Streams  
22 to Imitation of Tool-Use and Communicative Gestures. *Cereb Cortex*. 2018;28(2):474-492.  
23 doi:10.1093/cercor/bhw383
- 24 16. FB W, PF F. Towards a bottom-up perspective on animal and human cognition. *Trends Cogn*  
25 *Sci*. 2010;14(5):201-207. doi:10.1016/j.tics.2010.03.003
- 26 17. Passingham R. How good is the macaque monkey model of the human brain? *Curr Opin*  
27 *Neurobiol*. 2009;19(1):6-11. doi:10.1016/j.conb.2009.01.002.
- 28 18. Rilling JK, Glasser MF, Jbabdi S, Andersson J, Preuss TM. Continuity, divergence, and the  
29 evolution of brain language pathways. *Front Evol Neurosci*. 2012;3(11).  
30 doi:10.3389/fnevo.2011.00011.
- 31 19. Gupta S, Sinha A. Gestural communication of wild bonnet macaques in the Bandipur National  
32 Park, Southern India. *Behav Processes*. 2019;168(103956).  
33 doi:10.1016/j.beproc.2019.103956.
- 34 20. Rossi M, Fornia L, Puglisi G. Assessment of the praxis circuit in glioma surgery to reduce the  
35 incidence of postoperative and long-term apraxia: a new intraoperative test. *J Neurosurg*.  
36 2018;130(1):17-27. doi:10.3171/2017.7.JNS17357.

- 1 21. Fornia L, Rossi M, Rabuffetti M. Direct Electrical Stimulation of Premotor Areas: Different  
2 Effects on Hand Muscle Activity during Object Manipulation. *Cereb Cortex*. 2020;30(1):391-  
3 405. doi:10.1093/cercor/bhz139
- 4 22. Fornia L, Rossi M, Rabuffetti M. Motor impairment evoked by direct electrical stimulation of  
5 human parietal cortex during object manipulation. *Neuroimage*. 2022;248(118839).  
6 doi:10.1016/j.neuroimage.2021.118839
- 7 23. Viganò L, Fornia L, Rossi M. Anatomic-functional characterisation of the human “hand-knob”:  
8 A direct electrophysiological study. *Cortex*. 2019;113:239-254.  
9 doi:10.1016/j.cortex.2018.12.011
- 10 24. Viganò L, Howells H, Rossi M. Stimulation of frontal pathways disrupts hand muscle control  
11 during object manipulation. *Brain*. 2022;145(4):1535-1550. doi:10.1093/brain/awab379
- 12 25. Viganò L, Howells H, Fornia L, et al. Negative motor responses to direct electrical stimulation:  
13 Behavioral assessment hides different effects on muscles. *Cortex*. 2021;137:194-204.
- 14 26. Simone L, Fornia L, Viganò L. Large scale networks for human hand-object interaction:  
15 Functionally distinct roles for two premotor regions identified intraoperatively. *Neuroimage*.  
16 2020;204(116215). doi:10.1016/j.neuroimage.2019.116215
- 17 27. Bello L, Gambini A, Castellano A. Motor and language DTI Fiber Tracking combined with  
18 intraoperative subcortical mapping for surgical removal of gliomas. *Neuroimage*.  
19 2008;39(1):369-382. doi:10.1016/j.neuroimage.2007.08.031
- 20 28. Bello L, Riva M, Fava E. Tailoring neurophysiological strategies with clinical context  
21 enhances resection and safety and expands indications in gliomas involving motor pathways.  
22 *Neuro Oncol*. 2014;16(8):1110-1128. doi:10.1093/neuonc/not327
- 23 29. Rossi M, Viganò L, Puglisi G. Targeting Primary Motor Cortex (M1) Functional Components  
24 in M1 Gliomas Enhances Safe Resection and Reveals M1 Plasticity Potentials. *Cancers*  
25 (*Basel*). 2021;2021;13(15):3808. doi:10.3390/cancers13153808
- 26 30. Rossi M, Puglisi G, Nibali MC, et al. Asleep or awake motor mapping for resection of  
27 perirolandic glioma in the nondominant hemisphere? Development and validation of a  
28 multimodal score to tailor the surgical strategy. *J Neurosurg*. 2021;136(1):16-29.
- 29 31. Viganò L, Callipo V, Lamperti M, et al. Transcranial versus direct electrical stimulation for  
30 intraoperative motor-evoked potential monitoring: Prognostic value comparison in asleep  
31 brain tumor surgery. *Front Oncol*. 2022;12:1-10.
- 32 32. Puglisi G, Howells H, Sciortino T. Frontal pathways in cognitive control: direct evidence from  
33 intraoperative stimulation and diffusion tractography. *Brain*. 2019;142(8):2451-2465.  
34 doi:10.1093/brain/awz178

- 1 33. Puglisi G, Sciortino T, Rossi M. Preserving executive functions in nondominant frontal lobe  
2 glioma surgery: an intraoperative tool. *J Neurosurg.* 2018;131(2):474-480.  
3 doi:10.3171/2018.4.JNS18393
- 4 34. M CN, A L, G P. Preserving Visual Functions During Gliomas Resection: Feasibility and  
5 Efficacy of a Novel Intraoperative Task for Awake Brain Surgery. *Front Oncol.*  
6 2020;10(1485). doi:10.3389/fonc.2020.01485
- 7 35. Leonetti A, Puglisi G, Rossi M. Factors Influencing Mood Disorders and Health Related  
8 Quality of Life in Adults With Glioma: A Longitudinal Study. *Front Oncol.* 2021;11(662039).  
9 doi:10.3389/fonc.2021.662039
- 10 36. Lyle RC. A performance test for assessment of upper limb function in physical rehabilitation  
11 treatment and research. *Int J Rehabil Res.* 1981;4(4):483-492. doi:10.1097/00004356-  
12 198112000-00001
- 13 37. Yozbatiran N, Der-Yeghiaian L, Cramer SC. A standardized approach to performing the action  
14 research arm test. *Neurorehabil Neural Repair.* 2008;22(1):78-90.  
15 doi:10.1177/1545968307305353
- 16 38. Barbieri C, Renzi E. The executive and ideational components of apraxia. *Cortex.*  
17 1988;24(4):535-543. doi:10.1016/s0010-9452(88)80047-9
- 18 39. E R, F M, gestures NPI. A quantitative approach to ideomotor apraxia. *Arch Neurol.*  
19 1980;37(1):6-10. doi:10.1001/archneur.1980.00500500036003
- 20 40. Rorden C, Brett M. Stereotaxic display of brain lesions. *Behav Neurol.* 2000;12(4):191-200.  
21 doi:10.1155/2000/421719
- 22 41. Zhang Y, Kimberg DY, Coslett HB, Schwartz MF, Wang Z. Multivariate lesion-symptom  
23 mapping using support vector regression. *Hum Brain Mapp.* 2014;35(12):5861-5876.  
24 doi:10.1002/hbm.22590
- 25 42. DeMarco AT, Turkeltaub PE. A multivariate lesion symptom mapping toolbox and  
26 examination of lesion-volume biases and correction methods in lesion-symptom mapping.  
27 *Hum Brain Mapp.* 2018;39(11):4169-4182. doi:10.1002/hbm.24289
- 28 43. Wiesen D, Sperber C, Yourganov G, Rorden C, Karnath HO. Using machine learning-based  
29 lesion behavior mapping to identify anatomical networks of cognitive dysfunction: Spatial  
30 neglect and attention. *Neuroimage.* 2019;201:116000. doi:10.1016/j.neuroimage.2019.07.013
- 31 44. Königsberg A, DeMarco AT, Mayer C, et al. Influence of stroke infarct location on quality of  
32 life assessed in a multivariate lesion-symptom mapping study. *Sci Rep.* 2021;11(1):13490.  
33 doi:10.1038/s41598-021-92865-x
- 34 45. Mandal AS, Fama ME, Skipper-Kallal LM, DeMarco AT, Lacey EH, Turkeltaub PE. Brain  
35 structures and cognitive abilities important for the self-monitoring of speech errors. *Neurobiol*  
36 *Lang (Camb).* 2020;1(3):319-338. doi:10.1162/nol\_a\_00015

- 1 46. Tadel F, Baillet S, Mosher JC, Pantazis D, Leahy RM. Brainstorm: a user-friendly application  
2 for MEG/EEG analysis. *Comput Intell Neurosci.* 2011;2011(879716).  
3 doi:10.1155/2011/879716
- 4 47. Orban GA. Functional definitions of parietal areas in human and non-human primates. *Proc*  
5 *Biol Sci.* 2016;13;283(1828):20160118. doi:10.1098/rspb.2016.0118.
- 6 48. van Grinsven EE, Smits AR, van Kessel E, et al. The impact of etiology in lesion-symptom  
7 mapping - A direct comparison between tumor and stroke. *Neuroimage Clin.* 2023;37:103305.  
8 doi:10.1016/j.nicl.2022.103305
- 9 49. Siddiqi SH, Kording KP, Parvizi J, Fox MD. Causal mapping of human brain function. *Nat*  
10 *Rev Neurosci.* 2022;23(6):361-375. doi:10.1038/s41583-022-00583-8
- 11 50. Sperber C, Wiesen D, Karnath HO. An empirical evaluation of multivariate lesion behaviour  
12 mapping using support vector regression. *Hum Brain Mapp.* 2019;40(5):1381-1390.  
13 doi:10.1002/hbm.24476
- 14 51. Liepmann H. *Drei Aufsätze aus dem Apraxiegebiet.* Karger; 1908.
- 15 52. Lesourd M, Osiurak F, Baumard J, Bartolo A, Vanbellingen T, Reynaud E. Cerebral correlates  
16 of imitation of intransitive gestures: An integrative review of neuroimaging data and brain  
17 lesion studies. *Neurosci Biobehav Rev.* 2018;95:44-60. doi:10.1016/j.neubiorev.2018.07.019
- 18 53. Andersen RA, Andersen KN, Hwang EJ, Hauschild M. Optic ataxia: from Balint's syndrome  
19 to the parietal reach region. *Neuron.* 2014;81(5):967-983. doi:10.1016/j.neuron.2014.02.025
- 20 54. Bosco A, Bertini C, Filippini M, Foglino C, Fattori P. Machine learning methods detect arm  
21 movement impairments in a patient with parieto-occipital lesion using only early kinematic  
22 information. *J Vis.* 2022;22(10). doi:10.1167/jov.22.10.3
- 23 55. Karnath HO, Perenin MT. Cortical control of visually guided reaching: evidence from patients  
24 with optic ataxia. *Cereb Cortex.* 2005;15(10):1561-1569. doi:10.1093/cercor/bhi034
- 25 56. Binkofski F, Buxbaum LJ. Two action systems in the human brain. *Brain Lang.*  
26 2013;127(2):222-229. doi:10.1016/j.bandl.2012.07.007
- 27 57. Sakreida K, Effnert I, Thill S, et al. Affordance processing in segregated parieto-frontal dorsal  
28 stream sub-pathways. *Neurosci Biobehav Rev.* 2016;69:89-112.  
29 doi:10.1016/j.neubiorev.2016.07.032
- 30 58. Orban GA, Lanzilotto M, Bonini L. From Observed Action Identity to Social Affordances.  
31 *Trends Cogn Sci.* 2021;25(6):493-505. doi:10.1016/j.tics.2021.02.012
- 32 59. Turella L, Rumiati R, Lingnau A. Hierarchical Action Encoding Within the Human Brain.  
33 *Cereb Cortex.* 2020;30(5):2924-2938. doi:10.1093/cercor/bhz284

- 1 60. Bartolo A, Cubelli R, Della Sala S, Drei S, Marchetti C. Double dissociation between  
2 meaningful and meaningless gesture reproduction in apraxia. *Cortex*. 2001;37(5):696-699.  
3 doi:10.1016/s0010-9452(08)70617-8
- 4 61. Tessari A, Canessa N, Ukmar M, Rumiati RI. Neuropsychological evidence for a strategic  
5 control of multiple routes in imitation. *Brain*. 2007;130(Pt 4):1111-1126.  
6 doi:10.1093/brain/awm003
- 7 62. Rothi LJ, Ochipa C, Heilman KM. A cognitive neuropsychological model of limb praxis.  
8 *Cognitive Neuropsychology*. 1991;8(6):443-458. doi:10.1080/02643299108253382
- 9 63. Lanzilotto M, Ferroni CG, Livi A. Anterior Intraparietal Area: A Hub in the Observed  
10 Manipulative Action Network [published correction appears in *Cereb Cortex*. *Cereb Cortex*.  
11 2020;10;30(1):100. doi:10.1093/cercor/bhz011
- 12 64. Lanzilotto M, Maranesi M, Livi A, Ferroni CG, Orban GA, Bonini L. Stable readout of  
13 observed actions from format-dependent activity of monkey's anterior intraparietal neurons.  
14 *Proc Natl Acad Sci U S A*. 2020;117(28):16596-16605. doi:10.1073/pnas.2007018117
- 15 65. Aflalo T, Zhang CY, Rosario ER, Pouratian N, Orban GA, Andersen RA. A shared neural  
16 substrate for action verbs and observed actions in human posterior parietal cortex. *Sci Adv*.  
17 2020;2020;6(43):eabb3984. doi:10.1126/sciadv.abb3984
- 18 66. Króliczak G, Piper BJ, Frey SH. Atypical lateralization of language predicts cerebral  
19 asymmetries in parietal gesture representations. *Neuropsychologia*. 2011;49(7):1698-1702.  
20 doi:10.1016/j.neuropsychologia.2011.02.044
- 21 67. Johnson-Frey SH. The neural bases of complex tool use in humans. *Trends Cogn Sci*.  
22 2004;8(2):71-78. doi:10.1016/j.tics.2003.12.002
- 23 68. Pulvermüller F. How neurons make meaning: brain mechanisms for embodied and abstract-  
24 symbolic semantics. *Trends Cogn Sci*. 2013;17(9):458-470. doi:10.1016/j.tics.2013.06.004
- 25 69. Binder D JR, R.H. The neurobiology of semantic memory. *Trends Cogn Sci*. 2011;15(11):527-  
26 536. doi:10.1016/j.tics.2011.10.001
- 27 70. Power JD, Schlaggar BL, Lessov-Schlaggar CN, Petersen SE. Evidence for hubs in human  
28 functional brain networks. *Neuron*. 2013;79(4):798-813. doi:10.1016/j.neuron.2013.07.035
- 29 71. Borghi AM, Riggio L. Stable and variable affordances are both automatic and flexible. *Front*  
30 *Hum Neurosci*. 2015;9:351. doi:10.3389/fnhum.2015.00351
- 31 72. Assem M, Glasser MF, Essen DC, Duncan J. A Domain-General Cognitive Core Defined in  
32 Multimodally Parcellated Human Cortex. *Cereb Cortex*. 2020;30(8):4361-4380.  
33 doi:10.1093/cercor/bhaa023
- 34 73. Duncan J. The multiple-demand (MD) system of the primate brain: mental programs for  
35 intelligent behaviour. *Trends Cogn Sci*. 2010;14(4):172-179. doi:10.1016/j.tics.2010.01.004

## 1 **Figure legends**

2 **Figure 1 Schematic representation of the workflow of the study.**

3

4 **Figure 2 Resection Cavities overlap and scores.** A) Overlapping map of patients' resection  
5 cavities; B) distribution of De Renzi and C) ARAT scores and pre/post-surgery statistical results.

6

7 **Figure 3 SVR-LSM results.** A) SVR-LSM results for the ARAT global score covariate with the  
8 De Renzi global score. B) SVR-LSM results for the De Renzi global score covariate with the  
9 ARAT global score and SVR-LSM results for Meaningless and Meaningful gestures both  
10 covariate for the ARAT global score. C) Overlap between ARAT and De Renzi covariate CFWER  
11 clusters with HCP-MMP1 parietal regions. D) Overlap between ARAT and De Renzi CFWER  
12 covariate results and common region resulting from overlap of non-covariate CFWER results.

13

14 **Figure 4 Spatial matching between DES and SVR-LSM results.** A) HMt and sampling of  
15 parietal stimulation from Fornia et al. 2021. B(i-ii) Co-localization between HMt probability  
16 density estimation (effective areas in white and ineffective areas in black), praxis cluster (red) and  
17 prehension-praxis common region (orange). On the upper part of B(i), examples of EMG  
18 interference patterns evoked by parietal DES of phAIP and PF. B(iii) HMt probability maps  
19 showing the parietal region associated to different EMG-interference pattern (task-clumsy vs task-  
20 arrest) regardless ineffective sites. B(iiii) Co-localization between HMt task-arrest and clumsy  
21 pattern probability with meaningful (blue), meaningless (red) gestures CFWER (covariate ARAT)  
22 and posterior parietal regions (phAIP, DIPSA, DIPSM, PF). C(i) Anatomical localization of  
23 effective sites recorded within the parietal white matter. C(ii) Probability density estimation of  
24 HMt effective sites within the white matter and their co-localization with Praxis CFWER  
25 (covariate ARAT). D) Example of two patients showing transient post-operative apraxia: A)  
26 effective site was located in the white matter below AIP and evoked a task-arrest pattern; B)  
27 effective sites were located in the white matter below PF and evoked task-clumsy patterns.

28

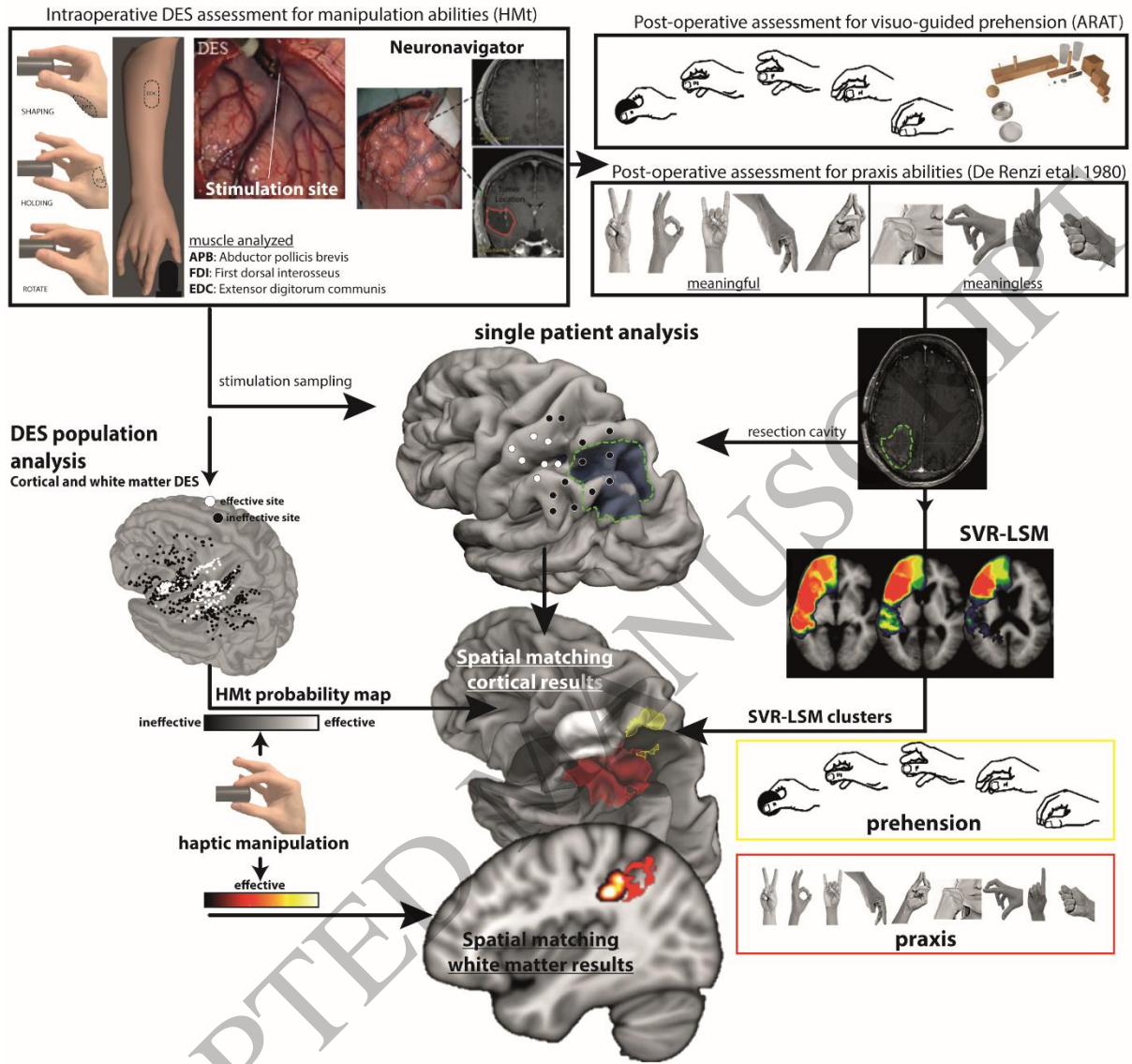


Figure 1  
159x152 mm (x DPI)

1  
2  
3  
4

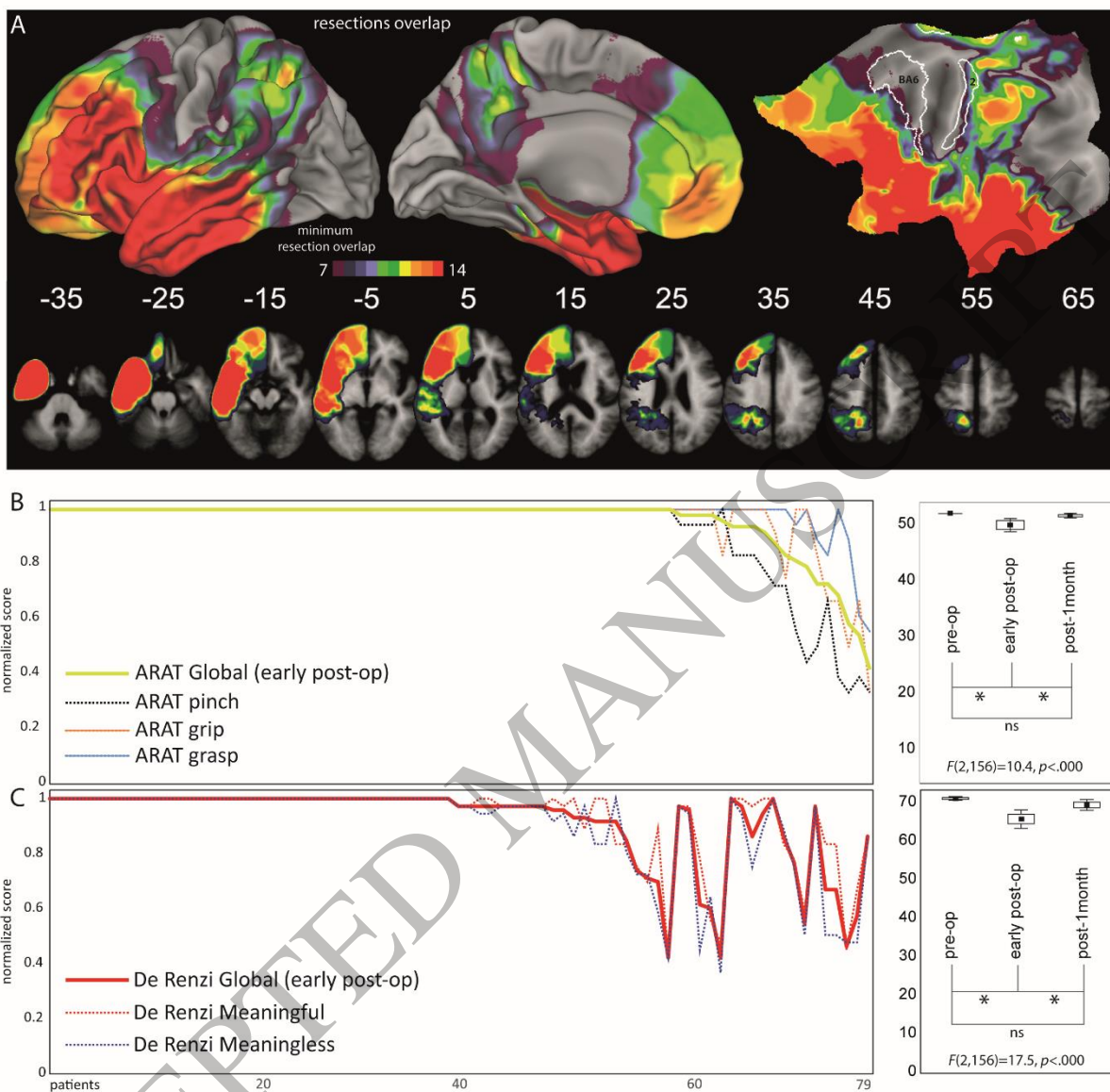


Figure 2  
159x159 mm ( x DPI)

1  
2  
3  
4



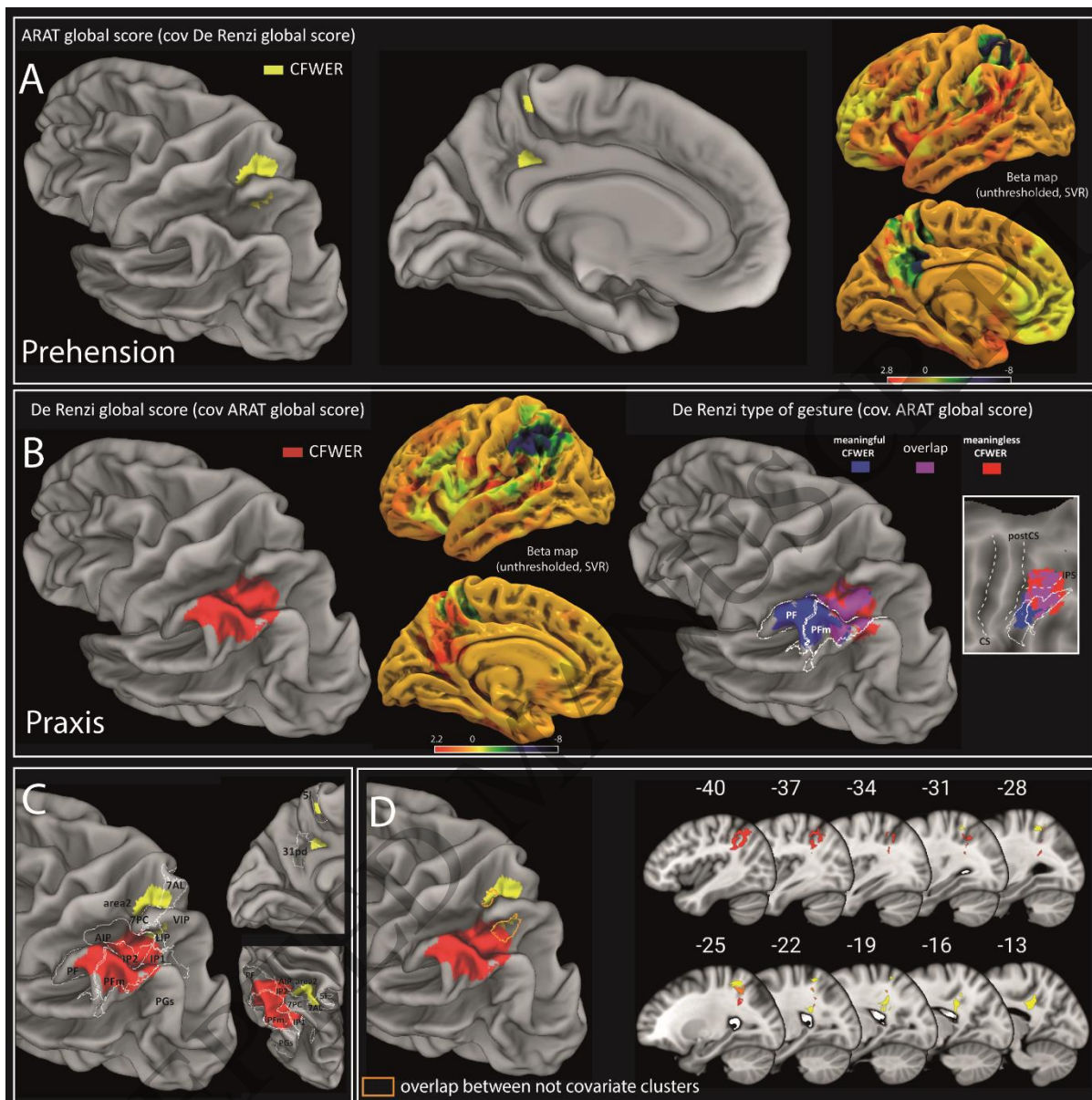


Figure 3  
159x159 mm (x DPI)

1  
2  
3  
4

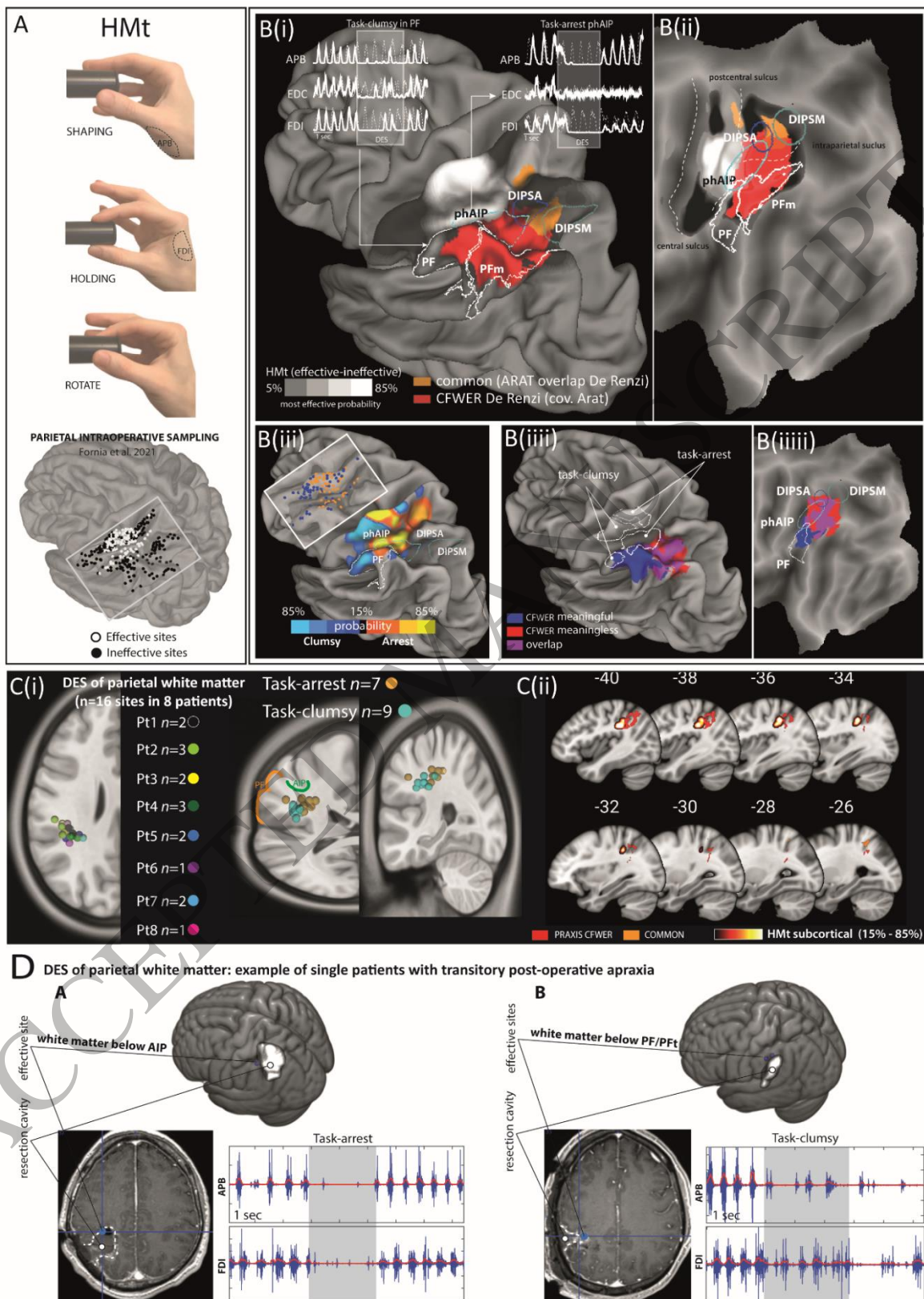


Figure 4  
159x225 mm (x DPI)

1  
2  
3